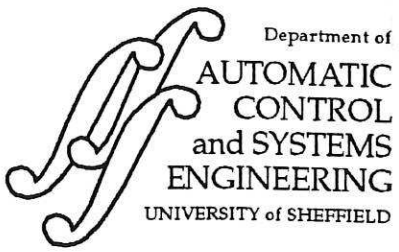


# CO-OPERATIVE CONTROL OF MULTIPLE ARMS MOUNTED ON A MOBILE PLATFORM

S.M. ZIAUDDIN and A.M.S. ZALZALA

*Robotics Research Group*
*Department of Automatic Control and Systems Engineering*
*The University of Sheffield*
*Mappin Street, Sheffield S1 3JD, United Kingdom*

Research Report #603
October 1995

Tel : +44 (0)114 2825250
Fax : +44 (0)114 2731729
EMail : rrg@sheffield.ac.uk
**Robotics Research Group**



# Cooperative Control of Multiple Arms Mounted on a Mobile Platform

S. M. Ziauddin and A. M. S. Zalzala

*Robotics Research Group, Department of Automatic Control and Systems Engineering, University of Sheffield, Mappin Street, Sheffield S1 3JD, United Kingdom.*

**Abstract**

*This paper is concerned with the control and cooperation of multiple arms mounted on a mobile platform. This represents a highly coupled and redundant system in which the motion of the arms affect that of the platform and vice versa. The objective is to develop control techniques to accurately track the motion of an object held jointly by a number of arms, while moving the platform along its desired trajectories as closely as possible. Moreover, the internal forces on the object are controlled to avoid damaging the object during manipulation. New dynamic and kinematic hybrid controllers are developed for the system. The dynamic controller is based on full model linearization while the kinematic controller utilises the concept of augmented Jacobian. The performance of the controllers is tested on a full scale simulator of two six-degrees-of-freedom PUMA arms mounted on a three-degrees-of-freedom platform.*

## 1. Introduction

Multi-arm systems have been proposed in the literature to expand the domain of operation of robots beyond the capabilities of single arms. Multiple arm systems can provide many financial benefits [2]. For instance, the application of a single robot in automating a task is typically achieved with intricate jigs or fixtures, which represent a significant fraction of the overall start-up cost. This means that whenever a new operation is implemented, much of the start-up cost must be incurred in the procurement of new peripheral devices. An alternative more flexible approach is the use of multi-arm robots which can perform as adaptable peripheral devices. Process cycle time can be reduced if multiple arms operate on the same work piece simultaneously. Expensive resources such as workspace and peripherals can be shared by multiple robots, thereby cutting down the overall cost. Optimum utilisation of robot capabilities may be possible in a multi-arm environment. For instance, a heavy duty robot can be made to behave like an adaptable vice holding a work-piece, while a precision robot operates on it. Handling of large and voluminous objects, that are beyond the capacity of a single arm, can become possible with multiple arms. Such potential applications make multi-arm control and coordination attractive, and has therefore been the focus of several studies [2, 3, 4, 6, 8, 10, 11, 12, 13].

Most recent studies, however, focus on fixed base manipulators. Fixed base systems unnecessarily restrict the work space volume of the arms, imposing limitations on the nature of jobs that could otherwise be possible if the arms were free to move. The problem is particularly acute in cooperating multiple arm systems as the workspace of such systems is considerably smaller than the sum of the workspaces of individual arms. The flexibility of a cooperative system can be enhanced by providing the arms with a certain degree of freedom of movement, thereby reducing cell size limitations. Such a system adds up the advantages of fixed base cooperating arms and mobile arms, and can be used in production lines or in places where large materials are to be carried over long distances that are beyond the reach of fixed base robots. This is particularly important in difficult or hazardous environments, where human intervention may not be available. Other applications include cooperative arms on remotely operated vehicles, autonomous and semi-autonomous loading / unloading and assembly robots, manipulators mounted on lar· ·ovable structures, and coordination of fingered articulated hands with the motion of the arm on which they are mounted. Moreover, the redundancy introduced by the motion of the base can be utilised in minimisation of joint torques or maximisation of manipulability of the system.

The review of the literature on multiple arm cooperation reveals that the aspect of platform mobility within a cooperative environment has not received much attention. Techniques for simulating cooperative arms on a mobile platform are discussed in [7], however, control aspects are not touched. Results of cooperative control of two-link SCARA arms mounted on a platform having unknown motion are given in [11].

This paper presents two hybrid control structures for controlling an arbitrary number of cooperative arms mounted on a mobile platform. Explicit control of the motion of the object held jointly by the arms, its internal forces, and the motion of the platform are achieved. The paper is organised as follows. Section 2

gives the model formulation of cooperative arms mounted on a mobile platform. A dynamic controller for the system is developed in section 3, while section 4 presents a kinematic controller. Simulation results of the two controllers are presented in section 5 and conclusions are drawn in section 6.

## 2. Dynamic Model Formulation

The primary emphasis in this work is on mobility of the arms as they handle a rigid object. Certain assumptions are made on the type of interaction between each arm and the object, and the number of degrees of freedom of each arm in the closed chain. The interaction between each arm and the object is restricted to a complete fixing by a gripper, so that each arm can exert three forces and three moments on the object. Cases of more general grasp types can be found elsewhere in the literature [6, 8, 13]. Each arm is rigid and has six degrees of freedom. Moreover, each arm is equipped with a force / torque sensor capable of measuring three orthogonal forces and three moments at the end-effector. It is further assumed that none of the manipulators experiences a singularity where its Jacobian becomes de-generate.

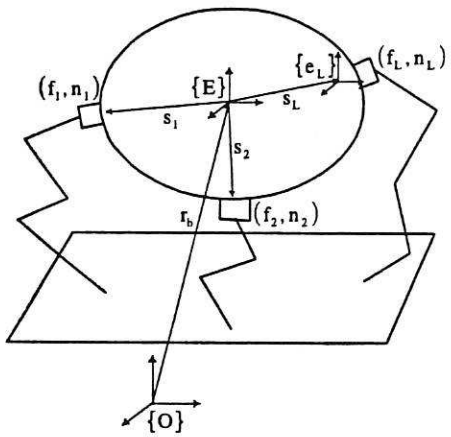


**Figure 1** Mobile multiple arm cooperation.

Consider Figure 1 which shows an object being manipulated by L arms mounted on a platform. Object coordinate frame {E} is fixed to the centre of mass of the object. A frame $\{e_i\}$ is fixed at the grasp point of the $i$th arm. Force $\mathbf{f}_{hi} \in \Re^{6\times1} = \left[\mathbf{f}_i^T \quad \mathbf{n}_i^T\right]^T$ is applied by the $i$th arm to the object at the origin of $\{e_i\}$, where $\mathbf{f}_i$ and $\mathbf{n}_i$ are its linear and angular components. The position of the object coordinate frame {E} with respect to the global reference frame {O} is given by $\mathbf{r}_b \in \Re^{3\times1}$ and its orientation is given by the rotation matrix $\mathbf{R}_E^O \in \Re^{3\times3}$. $\mathbf{s}_i \in \Re^{3\times1}$ is the displacement vector from the coordinate frame {E} to the coordinate frame $\{e_i\}$. The closed form dynamic equation of L six-linked manipulators, mounted on a $p$ degrees of freedom mobile platform is given by [7],

$$\mathbf{M}(\theta)\ddot{\theta} + \mathbf{h}(\theta,\dot{\theta}) + \mathbf{J}^T\mathbf{f}_h = \tau \qquad (1)$$

where $\mathbf{M} \in \Re^{(6L+p)\times(6L+p)}$ is the composite inertia matrix, $\mathbf{h} \in \Re^{(6L+p)\times1}$ is the composite Coriolis, centrifugal and gravitational force vector, $\tau \in \Re^{(6L+p)\times1}$ is the torque / force vector applied to each joint of the arm and the centre of mass of the platform, $\theta \in \Re^{(6L+p)\times1} = \left[\theta^{(b)T}\ \theta^{(1)T}\ \theta^{(2)T} \cdots\ \theta^{(L)T}\right]^T$ is the composite joint angle and platform configuration vector consisting of sub-parts $\theta^{(b)}$ and $\theta^{(i)}$, where $\theta^{(b)} \in \Re^{p\times1}$ is the vector representing the position and orientation of the platform, and $\theta^{(i)} \in \Re^{6\times1} = \left[\theta_1^{(i)}\ \theta_2^{(i)} \cdots \theta_6^{(i)}\right]^T$ is the joint angle vector of the $i$th arm. $\mathbf{J} \in \Re^{(6L)\times(6L+p)}$ is the composite Jacobian matrix of the system, and $\mathbf{f}_h \in \Re^{6L\times1} = \left[\mathbf{f}_{h1}^T\ \mathbf{f}_{h2}^T \cdots \mathbf{f}_{hL}^T\right]^T$ is the composite vector representing the external forces applied by all the end-effectors to the object. The object dynamic equations can be represented by the matrix equation

$$\mathbf{M}_b\mathbf{a}_b + \mathbf{q} = \mathbf{W}\mathbf{f}_h = \mathbf{f}_b \qquad (2)$$

in which $\mathbf{M}_b \in \Re^{6\times6} = \mathrm{diag}[m_b\mathbf{I}_3, \mathbf{I}_b]$, where $m_b$ is the mass of the object, $\mathbf{I}_b$ its inertia tensor, and $\mathbf{I}_3$ a $3\times3$ identity matrix. $\mathbf{a}_b \in \Re^{6\times1} = [\ddot{\mathbf{r}}_b^T\ \dot{\omega}_b^T]^T$ represents the object acceleration, $\mathbf{q} \in \Re^{6\times1} = [-m_b\mathbf{g}^T\ \{\omega_b \times \mathbf{I}_b\omega_b\}^T]^T$ where $\mathbf{g}$ represents acceleration due to gravity and $\omega_b$ is the angular velocity of the object and $\mathbf{f}_b \in \Re^{6\times1}$ is the force / moment applied to the object. $\mathbf{W} \in \Re^{6\times6L}$ is the Jacobian transformation from the object coordinate frame {E} to the arm tip frames $\{e_i\}$, and is given by

$$\mathbf{W} = \left[\mathbf{W}_1 \quad \mathbf{W}_2 \quad \cdots \quad \mathbf{W}_L\right] \qquad (3)$$

$$\mathbf{W}_i \in \Re^{6\times6} = \begin{bmatrix} \mathbf{I}_3 & \mathbf{0} \\ \mathbf{S}_i & \mathbf{I}_3 \end{bmatrix} \qquad (4)$$

$\mathbf{S}_i$ is defined so that its product with a vector $\mathbf{z}$ is equal to the vector cross-product given by $\mathbf{S}_i\mathbf{z} = \mathbf{s}_i \times \mathbf{z}$. As a result of the constraints imposed by the grippers on the motion of the end-effectors the following equation holds

$$\mathbf{a}_h = \mathbf{J}\ddot{\theta} + \dot{\mathbf{J}}\dot{\theta} = \mathbf{W}^T\mathbf{a}_b + \mathbf{a}_c \qquad (5)$$

where $\mathbf{a}_h \in \Re^{6L\times1} = [\mathbf{a}_{h1}^T\ \mathbf{a}_{h2}^T \cdots \mathbf{a}_{hL}^T]^T$ is the composite vector of end-effector accelerations and $\mathbf{a}_c \in \Re^{6L\times1} = \left[\mathbf{a}_{c1}^T\ \mathbf{a}_{c2}^T\ \cdots\ \mathbf{a}_{cL}^T\right]^T$ in which $\mathbf{a}_{ci} \in \Re^{6\times1} = \left[\{\omega_b \times (\omega_b \times \mathbf{s}_i)\}^T\ \mathbf{0}^T\right]^T$. To computed the forward dynamics of the system, equations (1), (2) and (5) can be solved together to calculate the end-effector forces

$$\mathbf{f}_h = (\mathbf{W}^T\mathbf{M}_b^{-1}\mathbf{W} + \mathbf{J}\mathbf{M}^{-1}\mathbf{J}^T)^{-1}\{\mathbf{J}\mathbf{M}^{-1}(\boldsymbol{\tau} - \mathbf{h}) + \mathbf{W}^T\mathbf{M}_b^{-1}\mathbf{q} - \mathbf{a}_c + \dot{\mathbf{J}}\dot{\boldsymbol{\theta}}\} \quad (6)$$

which are substituted into (1) to get the joint and platform acceleration.

## 3. Dynamic Hybrid Controller

The control structure is divided into motion and internal force control parts. The kinematic relationship between the composite arm tip velocity vector and the composite joint and platform velocity vector is given by

$$\mathbf{v}_h = \mathbf{J}(\boldsymbol{\theta})\dot{\boldsymbol{\theta}} \quad (7)$$

where $\mathbf{v}_h \in \Re^{6L\times 1} = \left[\mathbf{v}_{h1}^T\ \mathbf{v}_{h2}^T \cdots \mathbf{v}_{hL}^T\right]^T$ is the composite arm tip velocity vector and $\mathbf{v}_{hi} \in \Re^{6\times 1} = \left[\mathbf{v}_i^T\ \boldsymbol{\omega}_i^T\right]^T$ is the velocity of the $i$th end-effector. $\mathbf{J}$ is the composite Jacobian that has the general form

$$\mathbf{J} \in \Re^{(6L)\times(6L+p)} = \begin{bmatrix} \mathbf{J}_{1b} & \mathbf{J}_1 & \mathbf{0} & \cdots & \cdots & \mathbf{0} \\ \mathbf{J}_{2b} & \mathbf{0} & \mathbf{J}_2 & \mathbf{0} & \cdots & \mathbf{0} \\ \vdots & \vdots & \ddots & \ddots & \ddots & \vdots \\ \vdots & \vdots & & \ddots & \ddots & \mathbf{0} \\ \mathbf{J}_{Lb} & \mathbf{0} & \cdots & \cdots & \mathbf{0} & \mathbf{J}_L \end{bmatrix} \quad (8)$$

in which $\mathbf{J}_{ib} \in \Re^{6\times p}$ is responsible for the motion of the $i$th arm end-effector due to the motion of the platform, while $\mathbf{J}_i \in \Re^{6\times 6}$ is the Jacobian of the $i$th arm as if the arm was placed on a fixed platform. The composite Jacobian matrix $\mathbf{J}$ has a rectangular structure indicating the redundancy of the system. For the motion control part, the generalised inverse or the pseudo-inverse of $\mathbf{J}$ can be utilised to compute the desired accelerations of the system as discussed in [13]. However, this approach does not provide explicit control over the motion of the platform. Moreover, computing the pseudo-inverse in each control cycle is an additional burden to the computing device. Because of the above reasons $\mathbf{J}$ is divided into sub-parts related to individual arms, and the controller equations are formulated in terms of individual arm Jacobians. From equation (8), $\mathbf{v}_{hi}$ is related to the joint velocity of the $i$th arm and the platform velocity by the equation

$$\mathbf{v}_{hi} = \mathbf{J}_i'\dot{\boldsymbol{\theta}}'^{(i)} \quad (9)$$

where $\dot{\boldsymbol{\theta}}'^{(i)} \in \Re^{(6+p)\times 1} = \left[\dot{\boldsymbol{\theta}}^{(b)T}\ \dot{\boldsymbol{\theta}}^{(i)T}\right]^T$ and $\mathbf{J}_i' \in \Re^{6\times(6+p)} = \left[\mathbf{J}_{ib}\ \mathbf{J}_i\right]$. $\mathbf{J}_i'$ is a rectangular matrix which indicates that each cooperating arm, when combined with the platform, constitutes a redundant system. Equation (9) can be written as

$$\mathbf{v}_{hi} = \mathbf{J}_{ib}\dot{\boldsymbol{\theta}}^{(b)} + \mathbf{J}_i\dot{\boldsymbol{\theta}}^{(i)} \quad (10)$$

Thus the $i$th arm joint velocity can be expressed in terms of the hand velocities and the platform velocities as given below

$$\dot{\boldsymbol{\theta}}^{(i)} = \mathbf{J}_i^{-1}\mathbf{v}_{hi} - \mathbf{J}_i^{-1}\mathbf{J}_{ib}\dot{\boldsymbol{\theta}}^{(b)} \quad (11)$$

A similar relationship between the joint accelerations and the end-effector / platform accelerations is given by

$$\ddot{\boldsymbol{\theta}}^{(i)} = \mathbf{J}_i^{-1}\mathbf{a}_{hi} - \mathbf{J}_i^{-1}\mathbf{J}_{ib}\ddot{\boldsymbol{\theta}}^{(b)} - \mathbf{J}_i^{-1}\dot{\mathbf{J}}_{ib}\dot{\boldsymbol{\theta}}^{(b)} - \mathbf{J}_i^{-1}\dot{\mathbf{J}}_i\dot{\boldsymbol{\theta}}^{(i)} \quad (12)$$

Equation (12) shows that for specified end-effector and platform accelerations, the required joint accelerations of the $i$th arm can be computed at the current states $(\boldsymbol{\theta}, \dot{\boldsymbol{\theta}})$ of the system. Corresponding to any specified object acceleration, the $i$th end-effector acceleration can be computed using equation (5). Then equation (12) can be used to compute $\ddot{\boldsymbol{\theta}}^{(i)}$ for all the arms, which along with $\ddot{\boldsymbol{\theta}}^{(b)}$ can be input to the dynamic model to compute the required torques / forces. However, The position and orientation of the object frame {E} with respect to {O} are given by the vector $\mathbf{x}_b \in \Re^{6\times 1} = \left[\mathbf{r}_b^T\ \ \boldsymbol{\delta}^T\right]^T$, where $\boldsymbol{\delta} = \left[\varphi\ \ \gamma\ \ \psi\right]^T$ is the Euler angle vector. The object acceleration is therefore given by

$$\mathbf{a}_b = \mathbf{A}\ddot{\mathbf{x}}_b + \dot{\mathbf{A}}\dot{\mathbf{x}}_b \quad (13)$$

where $\mathbf{A} = \mathrm{diag}[\mathbf{I}_3\ \mathbf{A}_\delta]$ and $\mathbf{A}_\delta$ for the Eulerian angles [1] is given by

$$\mathbf{A}_\delta = \begin{bmatrix} 0 & \mathrm{Cos}(\varphi) & \mathrm{Sin}(\gamma)\mathrm{Sin}(\psi) \\ 0 & \mathrm{Sin}(\varphi) & -\mathrm{Sin}(\gamma)\mathrm{Cos}(\varphi) \\ 1 & 0 & \mathrm{Cos}(\gamma) \end{bmatrix} \quad (14)$$

The equations for the dynamic motion controller are summarised below, in which the subscript 'des' refers to the desired values

$$\mathbf{a}_{b\,des} = \mathbf{A}\ddot{\mathbf{x}}_{b\,des} + \dot{\mathbf{A}}\dot{\mathbf{x}}_b \quad (15)$$

$$\mathbf{a}_{h\,des} = \mathbf{W}^T\mathbf{a}_{b\,des} + \mathbf{a}_c \quad (16)$$

$$\ddot{\boldsymbol{\theta}}_{des}^{(i)} = \mathbf{J}_i^{-1}\mathbf{a}_{hi\,des} - \mathbf{J}_i^{-1}\mathbf{J}_{ib}\ddot{\boldsymbol{\theta}}_{des}^{(b)} - \mathbf{J}_i^{-1}\dot{\mathbf{J}}_{ib}\dot{\boldsymbol{\theta}}^{(b)} - \mathbf{J}_i^{-1}\dot{\mathbf{J}}_i\dot{\boldsymbol{\theta}}^{(i)} \quad (17)$$

$$\boldsymbol{\tau}_m = \mathbf{M}\ddot{\boldsymbol{\theta}}_{des} + \mathbf{h} \quad (18)$$

In order to cope with the modelling errors, $\ddot{\boldsymbol{\theta}}_{des}^{(b)}$ and $\ddot{\mathbf{x}}_{b\,des}$ in the control law are replaced by the following servo compensation terms

$$\mathbf{u}_1 = \ddot{\boldsymbol{\theta}}_{des}^{(b)} + \mathbf{K}_{v1}(\dot{\boldsymbol{\theta}}_{des}^{(b)} - \dot{\boldsymbol{\theta}}^{(b)}) + \mathbf{K}_{p1}(\boldsymbol{\theta}_{des}^{(b)} - \boldsymbol{\theta}^{(b)}) \quad (19)$$

$$\mathbf{u}_2 = \ddot{\mathbf{x}}_{b\,des} + \mathbf{K}_{v2}(\dot{\mathbf{x}}_{b\,des} - \dot{\mathbf{x}}_b) + \mathbf{K}_{p2}(\mathbf{x}_{b\,des} - \mathbf{x}_b) \quad (20)$$

where $\mathbf{K}_{vi}$ and $\mathbf{K}_{pi}$ are gain matrices.

If the object trajectory is specified, the required $\mathbf{f}_b$ is obtained from the object dynamics given in equation (2). The problem then is to select the required end-effector forces $\mathbf{f}_h$ to produce $\mathbf{f}_b$. There are multiple solutions to this problem. In general, certain

components of the forces and moments exerted by the end-effectors on the object cancel each other. These components contribute to the internal forces of the object, without causing any motion. Let $\mathbf{f}_h^E \in \Re^{6L\times 1}$ denote the affect of $\mathbf{f}_h$ at the origin of the object coordinate frame, and $\mathbf{W}_E \in \Re^{6\times 6L}$ denote the corresponding object Jacobian, then

$$\mathbf{f}_h^E = \overline{\mathbf{W}}\mathbf{f}_h \tag{21}$$

where

$$\overline{\mathbf{W}} \in \Re^{6L\times 6L} = \mathrm{diag}\left[\mathbf{W}_1 \quad \mathbf{W}_2 \quad \cdots \quad \mathbf{W}_L\right] \tag{22}$$

Thus

$$\mathbf{f}_b = \mathbf{W}_E\mathbf{f}_h^E = \mathbf{W}_E\overline{\mathbf{W}}\mathbf{f}_h \tag{23}$$

where $\mathbf{W}_E$ is given by

$$\mathbf{W}_E \in \Re^{6\times 6L} = \left[\mathbf{I}_6 \quad \mathbf{I}_6 \quad \cdots \quad \mathbf{I}_6\right] \tag{24}$$

with $\mathbf{I}_6$ being an identity matrix. One solution of equation (23) is given by

$$\begin{aligned}\mathbf{f}_h^E &= \frac{1}{L}\begin{bmatrix}\mathbf{I}_6\\ \mathbf{I}_6\\ \vdots\\ \mathbf{I}_6\end{bmatrix}\mathbf{f}_b + \begin{bmatrix}\mathbf{I}_6\\ \frac{-1}{L-1}\mathbf{I}_6\\ \vdots\\ \frac{-1}{L-1}\mathbf{I}_6\end{bmatrix}\mathbf{f}_{int} \\ &= \mathbf{W}_E^+\mathbf{f}_b + \mathbf{W}_{E\,null}\mathbf{f}_{int}\end{aligned} \tag{25}$$

where $\mathbf{f}_{int} \in \Re^{6\times 1}$ is the internal force vector and $\mathbf{W}_{E\,null}$ represents the null-space of $\mathbf{W}_E$. $\mathbf{f}_h^E$ is then mapped into the joint space by the Jacobian transformation to get the joint torques required to produce the object motion and the internal forces. The joint torque is given by

$$\tau_f = \mathbf{J}^T\left[\overline{\mathbf{W}}^{-1}\left\{\mathbf{W}_E^+\left(\mathbf{M}_b\mathbf{a}_b + \mathbf{q}\right) + \mathbf{W}_{E\,null}\mathbf{f}_{int\,des}\right\}\right] \tag{26}$$

To compensate for the modelling errors $\mathbf{f}_{int\,des}$ in equation (26) is replaced by

$$\mathbf{u}_3 = \mathbf{f}_{int\,des} + \mathbf{K}_i\int_0^t\left(\mathbf{f}_{int\,des} - \mathbf{f}_{int}\right)dt \tag{27}$$

where $\mathbf{K}_i$ is a gain matrix. The total torque delivered to the system by the dynamic controller is given by the sum of the torques generated by the motion controller and the force controller

$$\tau = \tau_m + \tau_f \tag{28}$$

## 4. Kinematic Hybrid Controller

In the kinematic control of the mobile cooperating arms, the Cartesian position / orientation errors of the held object are multiplied by suitable gains to compute a Cartesian force vector. This force can be thought of as a fictitious force in the Cartesian coordinates, which if applied to the object, will push the object in a direction opposite to the Cartesian position errors. This force is added to the internal force vector and the result is mapped through the Jacobian transpose operator to compute the equivalent joint torques. A concept of augmenting the Jacobian matrix **J** by a number of rows, in order to make it a square matrix, is adopted from the theory of configuration control of single redundant arms [9]. With the help of this augmented Jacobian matrix, the platform motion is incorporated into the control law. Gravity compensation of the arms and the object is the only model information used in the kinematic controller.

The control torque is divided into two parts

$$\tau = \tau_s + \tau_g \tag{29}$$

where $\tau_s \in \Re^{(6L+p)\times 1}$ is the component responsible for the object motion, the platform motion, the object gravity compensation and the internal forces on the object, while $\tau_g \in \Re^{(6L+p)\times 1}$ is the gravity compensation for the mobile multiple arm system. $\tau_s$ is written as

$$\tau_s = \mathbf{J}_{aug}^T\mathbf{f}_{aug} \tag{30}$$

where $\mathbf{J}_{aug} \in \Re^{(6L+p)\times(6L+p)}$ is the augmented Jacobian matrix and $\mathbf{f}_{aug} \in \Re^{(6L+p)\times 1} = \left[\mathbf{f}_h^T \quad \mathbf{f}_p^T\right]^T$ is the augmented force vector, which includes $\mathbf{f}_h$ the composite end-effector force vector, and $\mathbf{f}_p \in \Re^{p\times 1}$ the force required to move the platform along its desired trajectory. $\mathbf{f}_h$ is given by

$$\mathbf{f}_h = \overline{\mathbf{W}}^{-1}\left[\mathbf{W}_E^+\left\{\mathbf{f}_m + \mathbf{f}_g\right\} + \mathbf{W}_{E\,null}\mathbf{f}_{int}\right] \tag{31}$$

where $\mathbf{f}_m \in \Re^{6\times 1}$ is the force due to the Cartesian motion errors, $\mathbf{f}_g \in \Re^{6\times 1}$ is the force due to gravity of the object, and $\mathbf{f}_{int} \in \Re^{6\times 1}$ is the internal force. $\mathbf{f}_m$ is generated by multiplying the Cartesian motion errors by suitable gain matrices

$$\mathbf{f}_m = \mathbf{K}_1\left(\Delta\mathbf{v}_b\right) + \mathbf{K}_2\left(\Delta\mathbf{x}_b\right) \tag{32}$$

where $\mathbf{K}_1$ and $\mathbf{K}_2$ are gain matrices and $\Delta\mathbf{v}_b$ and $\Delta\mathbf{x}_b$ represent the errors in the velocity and position / orientation of the object and can be computed as given in [5]. In order to compensate for the errors in the force loop, $\mathbf{f}_{int}$ in equation (31) is replaced by the integral servo terms given by

$$\mathbf{u} = \mathbf{f}_{int\,des} + \mathbf{K}_i\int_0^t\left(\mathbf{f}_{int\,des} - \mathbf{f}_{int}\right)dt \tag{33}$$

$\mathbf{f}_p$ is simply the servo errors of the platform given by

$$\mathbf{f}_p = \mathbf{K}_3\left(\theta_{des}^{(b)} - \theta^{(b)}\right) + \mathbf{K}_4\left(\dot{\theta}_{des}^{(b)} - \dot{\theta}^{(b)}\right) \qquad (34)$$

where $\mathbf{K}_3$ and $\mathbf{K}_4$ are appropriate gain matrices.

To form $\mathbf{J}_{aug}$, a set of kinematic functions that represents additional tasks to, be performed by a redundant system is chosen in Cartesian or joint space. Since controlling the position and orientation of the platform is one of the objectives, the platform variables are chosen to form the extra kinematic functions. Hence the kinematic functions are given by

$$\Gamma_i(\theta) = \theta_i^{(b)} \qquad i = 1 \cdots p \qquad (35)$$

The system Jacobian $\mathbf{J}$ is augmented with rows representing partial derivatives of the additional kinematic functions. This square augmented Jacobian is then used in place of the system Jacobian in the controller.

The augmented Jacobian matrix is therefore written as

$$\mathbf{J}_{aug} = \begin{bmatrix} \mathbf{J} \\ \mathbf{J}_{conf} \end{bmatrix} = \begin{bmatrix} \mathbf{J}_{1b} & \mathbf{J}_1 & \mathbf{0} & \cdots & \cdots & \mathbf{0} \\ \mathbf{J}_{2b} & \mathbf{0} & \mathbf{J}_2 & \mathbf{0} & \cdots & \mathbf{0} \\ \vdots & \mathbf{0} & \ddots & \ddots & & \vdots \\ \vdots & \vdots & \ddots & \ddots & \ddots & \mathbf{0} \\ \mathbf{J}_{Lb} & \vdots & & \ddots & \ddots & \mathbf{J}_L \\ \mathbf{I}_p & \mathbf{0} & \cdots & \cdots & \mathbf{0} & \mathbf{0} \end{bmatrix} \qquad (36)$$

where $\mathbf{J}_{conf} \in \Re^{(p)\times(6L+p)}$ is the part of the Jacobian due to the additional configuration variables, in which $\mathbf{I}_p$ is a $p \times p$ identity matrix.

## 5. Simulation Results

The two controllers are tested on a full scale simulator of two cooperating 6 DOF PUMA arms mounted on a 3 DOF platform. Because of space constraints some typical test results are presented in this section. Figure 2 shows a sequence of snap shots out of the animation results of the mobile cooperative arms. The objective is to cooperatively handle a rectangular block of mass 10 Kg while moving on a platform of mass 40 Kg. The desired trajectories of the object and the platform are shown in Figure 3. The internal forces / moments need to be kept at zero along each degree of freedom of the object. For the sake of simplicity, joints in each arm are numbered from 1 to 6. The control update frequency for both the controllers is fixed at 1 K.Hz.

For the dynamic controller ±30% errors are introduced in the inertia parameters of the controller with respect to the actual model. The trajectory tracking errors in the case of the dynamic controller are shown in Figure 4. During simulations of the dynamic controller, it was observed that the cooperative system remains stable

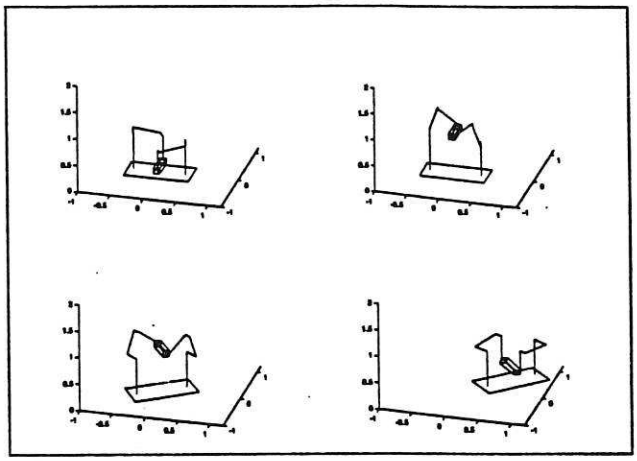

**Figure 2** Mobile cooperative manipulation snapshots.

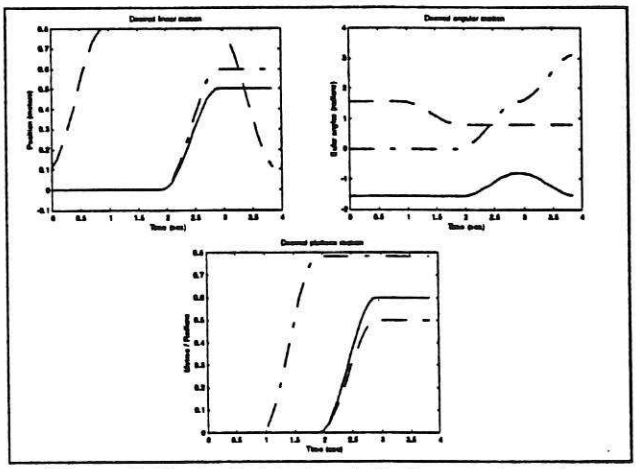

**Figure 3** Desired object and platform trajectories.

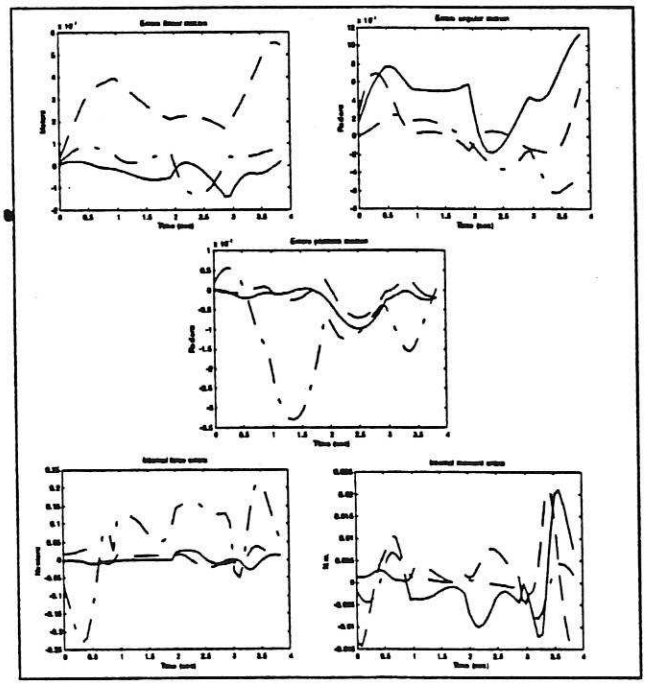

**Figure 4** Object / platform and $\mathbf{f}_{int}$ trajectory tracking errors in the case of dynamic hybrid control.

up to 50% inertia parameter errors and 120 Hz control update frequency. Therefore, these values represent limits within which inertia parameter errors and sampling frequencies should lie.

The kinematic controller was found to perform well at lower speeds. The results for the kinematic controller are plotted in Figure 5, where it must be noted that the speed of movement is four times reduced as compared to the earlier case. These figures show that despite low speed, the linear motion errors are larger than those of the dynamic controller. On the other hand the force response is satisfactory. During simulations it was noted that with kinematic control the system remained stable up to a control update frequency as low as 200 Hz.

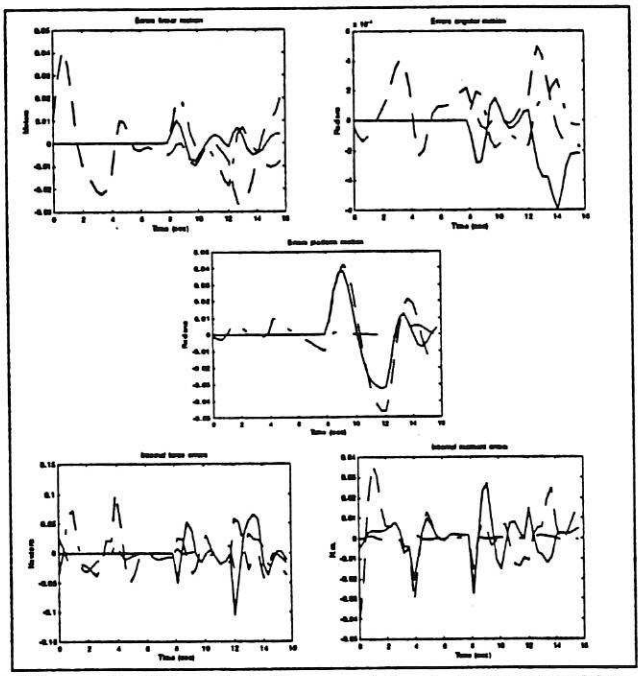

**Figure 5** Object / platform and $\mathbf{f}_{int}$ trajectory tracking errors in the case of kinematic hybrid control.

## 6. Conclusions

This paper presented two strategies for the control and cooperation of multiple mobile arms. A model based dynamic hybrid position / force controller was developed that linearized and decoupled the system, and achieved independent control over the motion of the held object and the platform. In this controller, the inversion of the composite Jacobian matrix was avoided by decomposing the Jacobian matrix into parts related to the individual arms. A relatively model independent, computationally efficient, kinematic controller was developed, where an extended Jacobian of the system was defined and was used to achieve motion tracking of the held object and the platform. Simulation results show that the inclusion of a model, despite ±30% errors in the parameters, improves position and force tracking compared to a kinematic controller, which performed well at low speeds, but its performance deteriorated at high speeds.

## References


1] Fu K.S., R.C. Gonzalez and C.S.G. Lee (1987). *Robotics Control, Sensing, Vision, and Intelligence*. McGraw-Hill, Inc.

2] Garg D.P. and R.F. Young (1990). Coordinated control of cooperating robotic manipulators. *Int. J. Systems Science*, Vol. 21, No. 11, pp. 2161-76.

3] Hayati S.A. (1988). Position and force control of coordinated multiple arms. *IEEE Trans. Aerospace and Electronic Systems*, Vol. 24, No. 5, pp. 584-590.

4] Kosuge K. and J. Ishikawa (1994). Task-oriented control of single-master multi-slave manipulator system. *Robotics and Autonomous Systems*, Vol. 12, part 1-2, pp. 95-105.

5] Luh J.Y.S., M.W. Walker and R.P. Paul (1980). Resolved acceleration control of mechanical manipulators. *IEEE Trans. Automatic Control*, Vol. AC-25, No. 3, pp. 468-474.

6] Mehrotra R., and M.R. Varanasi, (Ed.) (1990). *Multirobot Systems*. IEEE Computer Society Press.

7] Murphy S.H., J.T. Wen and G.N. Saridis (1991). Simulation of cooperating robot manipulators on a mobile platform. *IEEE Trans. Robotics and Automation*, Vol. 7, No. 4, pp. 468-478.

8] Ramadorai A.K., T.J. Tarn, A.K. Bejczy and N. Xi (1994). Task-driven control of multi-arm systems. *IEEE Trans. Control Systems Technology*, Vol. 2, No. 3, pp. 198-206.

9] Seraji H. (1989). Configuration control of redundant manipulators: theory and implementation. *IEEE Trans. Robotics Automation*, Vol. 5, No. 4, pp. 472-490.

10] Tarn T.J., A.K. Bejczy and X. Yun (1988). New nonlinear control algorithms for multiple robot arms. *IEEE Trans. Aerospace and Electronic Systems*, Vol. 24, No. 5, pp. 571-582.

11] Vasquez R.L. (1992). *Experiments in two-cooperating-arm manipulation from a platform with unknown motion*. Ph.D. Thesis, Stanford University, Department of Aeronautics and Astronautics, Stanford CA 94305.

12] Wen J.T. and K. Kreutz-Delgado (1992). Motion and force control of multiple robotic manipulators. *Automatica*, Vol. 28, No. 4, pp. 729-743.

13] Yoshikawa T. and X.Z. Zheng (1993). Coordinated dynamic hybrid position / force control for multiple robot manipulators handling one constrained object. *Int. J. Robotics Research*, Vol. 12, No. 3, pp. 219-230.